Published in final edited form as:
Ultrasound Med Biol. 2012 October ; 38(10): 1784–1798. doi:10.1016/j.ultrasmedbio.2012.06.013.

Investigating the efficacy of subharmonic aided pressure estimation for portal vein pressures and portal hypertension monitoring

Jaydev K. Dave[a,b], **Valgerdur G. Halldorsdottir**[a,b], **John R. Eisenbrey**[a], **Daniel A. Merton**[a], **Ji-Bin Liu**[a], **Jian-Hua Zhou**[a], **Hsin-Kai Wang**[a], **Suhyun Park**[c], **Scott Dianis**[c], **Carl L. Chalek**[c], **Feng Lin**[c], **Kai E. Thomenius**[c], **Daniel B. Brown**[a], and **Flemming Forsberg**[a]

[a]Department of Radiology, Thomas Jefferson University, Philadelphia, PA 19107, USA

[b]School of Biomedical Engineering, Science and Health Systems, Drexel University, Philadelphia, PA 19104, USA

[c]GE Global Research, Niskayuna NY 12309, USA

Abstract

The efficacy of using subharmonic emissions from Sonazoid microbubbles (GE Healthcare, Oslo, Norway) to track portal vein pressures and pressure changes was investigated in 14 canines using either slow- or high-flow models of portal hypertension (PH). A modified Logiq 9 scanner (GE Healthcare, Milwaukee, WI) operating in subharmonic mode ($f_{transmit}$:2.5MHz, $f_{receive}$:1.25MHz) was used to collect RF data at 10-40% incident acoustic power levels with 2-4 transmit cycles (in triplicate), before and after inducing PH. A pressure catheter (Millar Instruments, Inc., Houston, TX) provided reference portal vein pressures. At optimum insonification, subharmonic signal amplitude changes correlated with portal vein pressure changes; r ranged from -0.82 to -0.94 and from -0.70 to -0.73 for PH models considered separately or together, respectively. The subharmonic signal amplitudes correlated with absolute portal vein pressures (r: -0.71 to -0.79). Statistically significant differences between subharmonic amplitudes, before and after inducing PH, were noted ($p \leq 0.01$). Portal vein pressures estimated using SHAPE did not reveal significant differences ($p > 0.05$) with respect to the pressures obtained using the Millar pressure catheter. Subharmonic aided pressure estimation may be useful clinically for portal vein pressure monitoring.

Keywords

portal hypertension; subharmonic aided pressure estimation; noninvasive pressure estimation; ultrasound contrast agents; subharmonic imaging

Address all correspondence to: Flemming Forsberg, Ph.D., Department of Radiology, Thomas Jefferson University, Suite 763J, Main Building, 132 South 10th Street, Philadelphia, PA 19107, USA, Tel. (215) 955-4870, Fax (215) 955-8549, flemming.forsberg@jefferson.edu.

INTRODUCTION

Portal hypertension (PH) is defined as an absolute portal vein pressure above 6-10 mmHg or a pressure gradient between the portal vein and the hepatic vein or the inferior vena cava greater than 5 mmHg (Cokkinos and Dourakis 2009). Common complications associated with PH include ascites, encephalopathy and variceal bleeding with a high associated mortality (20 - 70 %) (D'Amico et al. 2006; Navarro et al. 2008; Sanyal et al. 2008). Clinical manifestations of PH occur only after severe liver dysfunction or cirrhosis have developed and thus, identifying nascent PH is imperative to limit associated morbidity and mortality (Halpern 2006; Moan 2009). An indirect measure of PH, the hepatic venous pressure gradient (HVPG), is the clinical standard (Lebrec et al. 1997). The HVPG is calculated as the difference between the wedged and free hepatic venous pressures by introducing a diagnostic catheter into the hepatic vein (Lebrec et al. 1997; Thabut et al. 2011). These clinically accepted HVPG measurements are invasive, are relatively expensive, require fluoroscopic guidance to guide the catheter and are not available in all centers. Thus a noninvasive technique, to measure HVPG or portal vein pressures directly would be of clinical value to assess PH. A noninvasive approach may also promote screening of patients suspected with liver diseases to gauge portal pressures or progression of cirrhosis.

Advancements in the field of ultrasound contrast agents (UCAs) including the production of stable encapsulated microbubbles and contrast specific imaging modes, have improved the sensitivity and specificity of diagnostic ultrasound (Goldberg et al. 2001; Iezzi et al. 2009; Dave et al. 2010; von Herbay et al. 2010). UCAs are encapsulated microbubbles that act as nonlinear scatterers of the incident ultrasound beam. This results in the emission of fundamental (f_0), subharmonic ($f_0/2$), harmonic ($n*f_0$; $n \in N$) and ultraharmonic ($((2n-1)/2)*f_0$; $n \in N \ \& \ n > 1$) components in the echo response (Goldberg et al. 2001). The nonlinear signals from UCAs have been used in clinical imaging applications, both in harmonic and subharmonic scanning modes with specifically tailored pulse sequences (Goldberg et al. 2001; Forsberg et al. 2007).

In addition to the imaging applications, various techniques to estimate ambient pressures using UCAs have been proposed (Miwa 1984; Fairbank and Scully 1977; Hök 1981; Shankar et al. 1986; Bouakaz et al. 1999). For example, techniques based on shift in the resonance frequency (Fairbank and Scully 1977), amplitude of single bubble echoes (Hök 1981), dual frequency excitations to calculate ambient pressure modulated size changes (Shankar et al. 1986), onset of ambient pressure modulated cavitations (Miwa 1984) and dissolution time of free microbubbles following rupture of encapsulated ones (Bouakaz et al. 1999). However, at best and under ideal *in vitro* conditions, these techniques yield resolution on the order of 10 to 50 mmHg, which is clinically unacceptable.

Alternatively, a technique to utilize subharmonic emissions from microbubbles to determine changes in ambient pressure called subharmonic aided pressure estimation (SHAPE) has been proposed (Shi et al. 1999). The subharmonic signal generation as a function of incident acoustic power (IAP), may be characterized into 3 stages – occurrence, growth and saturation (Shi et al. 1999; Shi et al. 2002). The concept of SHAPE revolves around the subharmonic signal emissions in the growth stage. In this stage, the subharmonic amplitude decreases linearly (in dB; $r^2 = 0.96$) with an increase in ambient pressure over a range of 0 to 186 mmHg (Shi et al. 1999). The first *in vivo* application of SHAPE was tested in canines using an invasive approach following mid-line incision to access the aorta and produced a maximum standard error of 5.4 mmHg relative to simultaneously recorded pressures by a Millar pressure catheter (Forsberg et al. 2005). However, this experimental setup was plagued by acquisition problems (employing 2 single element transducers held together with duct tape and no imaging capabilities), which is not clinically practical. Since then, other *in*

vitro (Adam et al. 2005; Ganor et al. 2005; Andersen and Jensen 2010; Frinking et al. 2010; Dave et al. 2011; Halldorsdottir et al. 2011) and *in vivo* (Dave et al. 2011; Dave et al. 2012a) applications of SHAPE have been documented. *In vitro* SHAPE investigations with six different commercial contrast agents determined that Sonazoid (GE Healthcare, Oslo, Norway) microbubbles (volume median diameter of 2.6 ± 0.1 μm; Sontum 2008) yielded the highest subharmonic change in response to changes in ambient pressures (Halldorsdottir et al. 2011). Also, the safety of Sonazoid for clinical applications has been established (Landmark et al. 2008) and Sonazoid is currently approved for diagnosis in patients with liver lesions in Japan (Bouakaz and de Jong 2007). *In vivo*, the use of Sonazoid microbubbles with SHAPE has been shown to track cardiac pressures in canines with errors in the range of 0.2 to 2.5 mmHg (Dave et al. 2012a).

Thus, the objective of this study was to investigate the efficacy of SHAPE with Sonazoid to track absolute portal vein pressures and changes in portal vein pressures when PH was induced in canines.

MATERIALS AND METHODS

Animal Preparation

This research study was approved by the Institutional Animal Care and Use Committee of Thomas Jefferson University and conducted in accordance with the guidelines provided by the National Institutes of Health. Fourteen canines were used in this study (mean weight: 22.5 ± 1.45 kg). Canines were selected for these studies on the basis of guidelines summarized for animal models of PH (Abraldes et al. 2006). The canines were fasted for a period of 24 hours prior to the experiments, to reduce post-prandial effects on portal vein pressures. Following an intravenous injection of Propofol (Abbott Laboratories, Chicago, IL; dose 7 ml/kg) the canines were placed on a warming blanket to maintain body temperature. The canines were intubated and anesthesia maintained with 0.5 to 2 % Isoflurane (Iso-thesia; Abbott Laboratories, Chicago, IL) via an endotracheal tube. An 18 gauge catheter was placed in a forelimb vein for Sonazoid infusion at a rate of 0.015 μl/kg/min (similar to other *in vivo* canine studies; Dave et al. 2011; Dave et al. 2012a). Throughout the experiment, the canines were monitored by certified veterinary technicians.

A midline abdominal incision was created to provide access to the main portal vein. A 5F pressure catheter (SPR 350S/ SPR 350, Millar Instruments, Inc., Houston, TX) was then introduced into the main portal vein to provide the reference pressures. An additional surgical inlet to the main portal vein was also created to induce PH (Fig. 1a). The location of the pressure catheter was verified by color Doppler ultrasound (Fig. 1b). Clinically, a modified form of Ohm's law for fluid flow ($\Delta P = Q \times R$; ΔP: change in pressure, Q: flow and R: resistance) models increases in portal vein pressures (Abraldes et al. 2006), either by an increase in portal vein flow or an increase in resistance to portal vein flow or a combination of these two. Thus, in this study two models of PH were adopted based on increase in resistance to portal vein flow and on increase in portal vein flow.

In a group of 8 canines, a slow flow (increased resistance) model of PH was induced by embolization of the liver microcirculation using Gelfoam (Ethicon, Somerville, NJ) injection. Gelfoam has been used in canines before (Mac and Matthews 1947) and has shown no foreign body reactions or inflammatory developments (Jenkins and Janda 1946). Approximately 2 to 3 sheets of Gelfoam were cut into small pieces and mixed with 4 ml to 5 ml of saline and then introduced into the portal vein via the surgical inlet. For the remaining 6 canines, an increased flow model of PH was induced surgically by connecting the splenic or the femoral artery to the portal vein using a 3-way stopcock with extension tube, thereby creating an arterial-venous (AV) fistula. An external saline infusion bag with a pressure

sensor and cuff were additionally used to increase the flow volume. For both these models of PH induction, the portal vein pressures were continuously monitored via the Millar pressure catheter. Following the experiments, the canines were sacrificed by intravenous injection of Beuthanasia (0.25 mg/kg).

Data Acquisition

The experimental setup is shown in Fig. 2. A Logiq 9 scanner (GE Healthcare, Milwaukee, WI) with a curved array 4C probe was modified to operate either in the standard imaging mode or in pulse inversion subharmonic imaging mode ($f_{transmit}$ = 2.5 MHz, $f_{receive}$ = 1.25 MHz; this choice of transmit and receive frequencies was based on our previous studies; Dave et al. 2011; Halldorsdottir et al. 2011; Dave et al. 2012a). A sonographer and a physician confirmed the presence of the pressure catheter in the portal vein and the patency of the portal vein using standard grayscale and/or color Doppler imaging. The 4C probe was positioned directly over the portal vein with sterile saline placed in the abdominal cavity to serve as a coupling medium and clamped to a support stand as illustrated in Fig. 2 to provide a constant scanning plane during the experiment. The sonographer and the physician monitored the ultrasound scanning plane and data acquisition with the clamped probe throughout the experiment. Using the ultrasound image as a guide, a region of interest (ROI) including the portal vein near the site of the pressure catheter was selected (Fig. 3a). The Logiq 9 scanner was then switched to RF data acquisition mode to acquire beamformed unfiltered RF data from the ROI (Fig. 3b). The pressure catheter was connected to an oscilloscope (Model 9350 AM, LeCroy, Chestnut Ridge, NY) through the transducer control unit (TCB 500, Millar Instruments). The oscilloscope was configured to acquire the pressure catheter data on a computer via a GPIB interface (Driver Version 2.7.0.49152) through LabVIEW (Version 8.0, National Instruments Corp., Austin, TX). A synchronization signal was obtained from the Logiq 9 scanner and was used to trigger the oscilloscope to acquire the pressure catheter data synchronously with the RF data acquisition (Fig. 2).

The performance of the SHAPE technique is dependent on the growth-stage subharmonic emissions, which in turn are dependent on the IAPs. The peak-negative acoustic pressures corresponding to the IAPs were measured at the focus of the transducer using a calibrated 0.2 mm needle hydrophone (Precision Acoustics, Dorchester, Dorset, UK; sensitivity of 57.1 mV/MPa at 2.5 MHz) in a water bath for each of the possible 28 IAP levels provided by the Logiq 9 scanner. The focal point was determined by finding the point of maximum acoustic pressure using a semi-automated electronic x-y-z positioning system and the measurements were performed in triplicate (the focal point depth was about 3.0 cm). The range of peak negative incident acoustic pressures spanned 0 to 0.58 MPa as the power output on the scanner was stepped from 0 to 100 %. Based on this data and previous *in vitro* and *in vivo* results showing “optimum” performance of SHAPE with Sonazoid to be in the range of 0.2 to 0.6 MPa (Shi et al. 1999; Dave et al. 2011; Halldorsdottir et al. 2011; Dave et al. 2012a), three IAP levels corresponding to 10 % (0.14 MPa; peak negative), 20 % (0.23 MPa; peak negative) and 40 % (0.36 MPa; peak negative) were selected. Minimal attenuation was expected *in vivo* due to intra-abdominal scanning. Higher IAPs (> 40 %) were avoided to prevent microbubble destruction. The confirmation that microbubble destruction did not occur below 40 % IAP was obtained using an *in vitro* flow phantom setup similar to the experimental setup used in previous studies (Dave et al. 2011). Lower IAPs (< 10 %) that elicit relatively low energy in the scattered beam profile at the subharmonic frequency were not used. Additionally, because the performance of SHAPE will vary with the number of transmit cycles used, 2, 3 and 4 transmit cycle pulses were considered, each at 10 %, 20 % and 40 % IAP levels.

Under baseline conditions (i.e., with normal portal vein pressures) after Sonazoid infusion and visual confirmation of Sonazoid microbubbles in the portal vein, the RF data and the

pressure catheter data were acquired synchronously with each combination of transmit cycles and IAP levels cumulating to 27 acquisitions (three acquisitions for every combination). Since the visibility of the ROI was compromised in the RF data acquisition mode (Fig. 3b), after every 3 acquisitions visual verification of the scanning plane and ROI were performed by the sonographer and the physician after switching the unit into imaging mode (Fig. 3a) and the ROI was relocated if required. After baseline conditions, the Sonazoid infusion was stopped and PH states were established using either Gelfoam or AV-fistula for the respective group of canines. Data acquisition in the PH states were again performed after initiating Sonazoid infusion for all transmit cycles and IAPs as described above. Note, that again 27 acquisitions were made (three acquisitions for each combination). The data were transferred to a computer for offline analyses in Matlab (Version 7.8.0-R2009a, The Mathworks, Inc., Natick, MA).

Data Processing

The data from each acquisition were saved as a DICOM file and the RF data extracted using a proprietary software 'GE Raw RF data extraction facility' (GE Global Research, Niskayuna NY). This RF data were DC filtered and then a filter centered at 1.25 MHz with 0.25 MHz bandwidth was applied to extract the subharmonic data (these filter parameters were selected based on previous *in vitro* results; Dave et al. 2011). The subharmonic data were log-compressed to generate maximum intensity image (MIP) (Fig. 4). An ROI_{PV} (PV: portal vein; to distinguish it from the ROI used to acquire the complete RF data) was used to select the region within the portal vein. The portal vein exhibited maximum subharmonic signal intensity from the presence of Sonazoid microbubbles, whereas there was suppression of tissue signals (because of no subharmonic generation in tissue) and cancellation of other linear signals in the field of view that result from the use of pulse inversion technique (as depicted in Fig. 4). These ROI_{PV} selections were made in consultation with the sonographer present during data acquisition stage. Based on the selected ROI_{PV}, the subharmonic signals were extracted as the mean subharmonic amplitude value obtained from the data corresponding to the MIP image (SH_{MIP}) as well as the mean subharmonic signal obtained from the ROI_{PV} data from all frames (SH_{All_Frames}). We included the data corresponding to the MIP images in our analyses, because the MIP images are useful in providing a snapshot of vasculature and thus, we wanted to verify if the data corresponding to the MIP images could be directly used for pressure estimation.

Statistical Analyses

For all statistical analyses p-values below 0.05 were considered significant. The subharmonic signal amplitudes were used to determine if there was a statistically significant difference between the number of transmit cycles and the subharmonic signal amplitude using a factorial repeated measures analysis of variance (ANOVA). Post hoc comparisons were performed after correcting for multiple comparisons based on the Bonferroni method (Bland and Altman 1995). Linear correlation analyses were performed to identify the relationship between change in the mean portal vein pressures and change in the subharmonic signal amplitude, and between absolute mean portal vein pressures and absolute subharmonic signal amplitudes. The correlation coefficients were compared based on calculated t-statistics (Field 2009). Paired t-tests were used to analyze the difference between baseline and PH conditions for portal vein pressures and subharmonic signal amplitudes.

A cross-validation study was also performed to estimate the errors obtained with the SHAPE technique. For the cross-validation study, data from one canine under baseline and PH was eliminated and, a linear model between subharmonic amplitude and the portal vein pressures was obtained using data from the remaining canines. Then, based on this linear model the

portal vein pressures at baseline and at PH condition were calculated for the canine not included in the linear model and compared to the pressure catheter data. Also based on the pressures obtained with this cross-validation approach, we calculated the sensitivity, specificity and the accuracy of identifying PH in these canines choosing a threshold value of 16 mmHg, because this represents the clinical scenario of HVPG values corresponding to moderate through severe PH cases. For canines, this value of 16 mmHg was selected based on data presented in literature (Seitchik et al. 1961, Yamana et al. 1983, Palmaz et al. 1986, Sugita et al. 1987, Chen et al. 2009, Jin et al. 2010, Buob et al. 2011).

All analyses were performed using IBM SPSS Statistics (Release 19.0.0; IBM Corporation, Armonk, NY).

RESULTS

Induced PH in Canines

The baseline mean portal vein pressure was 9.4 ± 2.1 mmHg (Table 1). For one canine from the Gelfoam group, technical difficulty associated with the pressure catheter impeded data acquisition and thus, the data from this canine were not included in the analyses. From the remaining 7 canines where PH was induced using Gelfoam, one canine did not respond to treatment (determined from the pressure catheter readings), thus post PH data was not acquired for this canine. Post-PH data for the remaining 6 canines in the Gelfoam group are shown in Table 1. From the group of 6 canines where PH was induced using AV-fistula, one canine did not respond to the treatment (no rise in portal vein pressures). No PH data were acquired from this canine and thus, portal vein data from the remaining 5 canines are shown in Table 1. As stated above, two canines (one from the Gelfoam group and one from the AV-fistula group) only provided baseline data. Instead, data from these 2 dogs were subsequently used to test the efficacy of the SHAPE technique in predicting portal vein pressures along with the cross-validation approach in other canines.

Subharmonic Amplitude as a Function of Number of Transmit Cycles and IAP Levels

Figure 5 shows a boxplot of the subharmonic signal amplitudes (SH_{MIP}) obtained from the portal veins. Note the relatively low subharmonic signal amplitude obtained with 2 transmit cycles (most probably due to the broad spectrum with 2 transmit cycles) and with 10 % IAP. A factorial repeated measures ANOVA used to compare the subharmonic signal amplitudes (both SH_{MIP} and SH_{All_Frames}) obtained from the portal vein (for baseline conditions) based on number of transmit cycles and IAP levels revealed a significant main effect of the number of transmit cycles ($F(1.10, 14.27) = 130.66$; $p < 0.001$) and of the IAPs ($F(1.15, 14.90) = 325.88$; $p < 0.001$). There was also a significant interaction effect between the number of transmit cycles and the IAP levels $F(1.35, 17.55) = 78.15$ ($p < 0.001$), indicating that the IAP levels had different effects on the subharmonic amplitude depending on the number of transmit cycles. Post hoc tests using Bonferroni adjustment for multiple comparisons showed that the subharmonic amplitude obtained with 2 transmit cycles was significantly less than the subharmonic amplitude with 3 (by 11.5 dB; 95 % Confidence Interval: 8.8 dB to 14.1 dB; $p < 0.001$) and with 4 (by 11.1 dB; 95 % Confidence Interval: 8.4 dB to 13.8 dB; $p < 0.001$) transmit cycles. However, there was no statistically significant difference between the subharmonic amplitudes obtained with 3 and 4 transmit cycles ($p = 0.498$). Thus, 2 transmit cycles may have lacked the ability to elicit a sufficient subharmonic response given the IAP levels considered in this study. Post hoc tests, again using Bonferroni adjustment for multiple comparisons, also showed that the subharmonic amplitude obtained with 10 % IAP was significantly less than the subharmonic amplitudes obtained with 20 % (by 7.7 dB; 95 % Confidence Interval: 6.4 dB to 8.9 dB; $p < 0.001$) and 40 % (by 11.3 dB; 95 % Confidence Interval: 9.7 dB to 13.0 dB; $p < 0.001$) IAPs. Hence, 10

% IAP at 2, 3, and 4 transmit cycles may not have sufficient power to elicit a subharmonic response detectable by the 4C probe used in this study. Figure 6 depicts subharmonic MIP images as a function of IAP levels and the number of transmit cycles obtained from one canine, before PH was induced. As seen in Fig. 6, the subharmonic signal amplitude was relatively low for 2 transmit cycles (Fig. 6a-c), with 3 transmit cycles the subharmonic signal amplitude gradually increased with an increase in IAP from 10 % to 40 % (Fig. 6d-f), then the subharmonic signal amplitude dropped for 10 % IAP and 4 transmit cycles (Fig. 6g), and finally the subharmonic signal amplitude increased for 20 % and 40 % IAP levels with 4 transmit cycles (Fig. 6h-i). Based on similar observations with data from other canines and the statistical analyses, it was concluded that the subharmonic signal at 10 % IAP and with 2 transmit cycles did not elicit the subharmonic signal in the growth-stage required for SHAPE application. Thus, only data obtained with 20 % and 40 % IAP levels with 3 and 4 transmit cycles were considered for further analyses.

Comparison of 3 and 4 Transmit Cycles for SHAPE Based PH Tracking

Figures 7 (3 cycle pulses) and 8 (4 cycles pulses) illustrate the relationship between the mean change in portal vein pressures (PH pressures – baseline portal vein pressures) and the mean change in the subharmonic signal amplitude (at PH state – at baseline conditions). Data obtained using the MIP image alone (SH_{MIP}; panels a and b) and obtained as an average of subharmonic signals from all the frames (SH_{All_Frames}; panels c and d) at 20 % (panels a and c) and at 40 % (panels b and d) IAP levels are shown in Figs. 7 and 8. As depicted in Fig. 7, for both models of PH when 3 transmit cycles were used, there was a reasonably good correlation (ranging from -0.62 to -0.81, n = 6 for the Gelfoam model and from -0.52 to -0.73, n = 5 for the AV-fistula model) between the change in subharmonic signal amplitude and change in portal vein pressures, with increased changes in portal vein pressures associated with increased changes in subharmonic signal. However, as shown in Fig. 8, when 4 transmit cycles were used, a relatively stronger correlation (ranging from -0.88 to -0.94, n = 6 for the Gelfoam model and from -0.82 to -0.83, n = 5 for the AV-fistula model) was observed. Table 2 presents the correlation coefficients observed with 3 and 4 transmit cycles at 20 % and 40 % IAP levels, when the data from both the PH models were combined (as a more robust indicator of SHAPE's performance). As seen in Table 2, significant and higher correlation coefficients were observed for 4 transmit cycles (*p*-values ranging from 0.01 to 0.02) as compared to 3 transmit cycles (*p*-values ranging from 0.07 to 0.1). This suggests that the use of 4 transmit cycles is preferred over 3 transmit cycles for SHAPE applications.

Comparison of 20 % and 40 % IAP Levels with 4 Transmit Cycles for SHAPE Based PH Tracking

There was no statistically significant difference ($p > 0.4$) between the correlation coefficients obtained with 20 % and 40 % IAP levels for 4 transmit cycles (c.f. Table 2). This suggests that at both these IAP levels the subharmonic emissions may be in the growth-phase and thus sensitive to ambient portal vein pressure changes. Additionally there was a strong significant correlation between the mean values of absolute subharmonic amplitudes and mean values of absolute portal vein pressures as documented in Table 3 and Fig. 9. This confirms that at both 20 % and 40 % IAP levels the subharmonic signal was in the ambient pressure sensitive phase. This result was consistent with evaluation of subharmonic MIP images (c.f. Fig. 6). As shown in Fig. 9a, the subharmonic signal amplitudes extracted from ROI_{PV} of all the frames (SH_{All_Frames}) were lower than the subharmonic signal amplitudes extracted from the MIP image (SH_{MIP}) (mostly due to some Sonazoid concentration fluctuations likely to happen *in vivo*). The gradients of the best-fit lines representing the sensitivity of Sonazoid microbubbles to ambient portal vein pressures ranged from -1.44 mmHg/dB to -1.69 mmHg/dB (Figs. 9a and 9c). Interestingly, the gradients for 20 % (Fig.

9a) and 40 % (Fig. 9c) IAPs were nearly independent of the technique used in analyzing the extracted subharmonic signals (either SH_{MIP} or SH_{All_Frames}). Also the gradient was lower for 20 % IAP as compared to 40 % IAP, indicating that the ambient pressure sensitivity was relatively more at 20 % IAP, with saturation most likely to occur above 40 % IAP. Figs. 9b and 9d show boxplots of subharmonic signals obtained before and after inducing PH, at 20 % and 40 % IAP levels with 4 transmit cycles, respectively. Note, that at baseline conditions (pre-PH) the spread in the subharmonic amplitudes is much less than the spread after PH (Figs. 9b and 9d), primarily because the portal vein pressures after induced PH also varied considerably between canines (see Table 1). A paired t-test comparing these subharmonic amplitudes revealed that there was a statistically significant difference between the subharmonic signal amplitudes obtained under baseline and under PH conditions at 20 % and 40 % IAPs (Table 4). Thus, subharmonic signal amplitudes may predict the portal vein pressures.

In order to test the viability of using subharmonic signal amplitudes to predict portal vein pressures, the subharmonic signal amplitudes obtained in 2 canines, where data were only obtained under baseline conditions were first analyzed. The subharmonic signal amplitudes were combined with the equation of the best fit line (shown in Figs. 9a and 9c) to predict the baseline portal vein pressures; the values were compared to the catheter pressures. These results are presented in Table 5 which demonstrate that the subharmonic signals analyzed from all the frames (SH_{All_Frames}) have relatively less error (error range: 0.2 to 1.9 mmHg) as compared to subharmonic signals analyzed only from the MIP image (SH_{MIP}; error range: 1.8 to 6.9 mmHg) in predicting portal vein pressures. This suggests that the subharmonic signal amplitude analyzed from all the frames (SH_{All_Frames}) is a more robust indicator of portal vein pressures and should be the most appropriate means to predict portal vein pressures; albeit based on analyses in 2 canines. Next, the results of the cross-validation study are summarized in Table 6 for the baseline and PH data compared together and also, independently. None of the differences between the pressures obtained using the catheter, and using the cross-validation approach and the SHAPE data were statistically significant ($p > 0.05$; Table 6). Finally, the results of the binary classification and the resulting sensitivity, specificity and accuracy of predicting PH are presented in Table 7.

DISCUSSION

The goal of this study was to analyze if subharmonic emissions from Sonazoid microbubbles (i.e., SHAPE) were useful in predicting portal vein pressures in canines. Subharmonic signals emitted in the growth stage have been shown to be useful for sensing ambient pressures (Shi et al. 1999). Thus, 3 IAP levels (10, 20 and 40 %) were considered. Also 2, 3, and 4 transmit cycles were evaluated to investigate their effect on SHAPE's performance in tracking portal vein pressures. Portal vein pressures were varied in canines using Gelfoam (slow flow model) or by a surgically created AV-fistula (high flow model) to induce PH. The canines' portal vein pressures were consistent with values reported in the literature (Sugita et al. 1987; Jin et al. 2010). Results showed that SHAPE performance in tracking PH was best with 4 transmit cycles for 20 % and 40 % IAP levels; the changes in portal vein pressures correlated with the changes in the subharmonic signal amplitudes for both cases, when the two PH models were evaluated separately (r ranging from -0.82 to -0.94; Fig. 8) and when evaluated together (r ranging from -0.70 to -0.73; Table 2). The subharmonic signal amplitude decreased with an increase in ambient pressure, which is consistent with previously published reports (Shi et al. 1999; Adam et al. 2005; Forsberg et al. 2005; Andersen and Jensen 2009; Andersen and Jensen 2010; Dave et al. 2011; Halldorsdottir et al. 2011; Dave et al. 2012a). Based on this result, the relationship between the absolute portal vein pressures and absolute subharmonic signal amplitudes were evaluated for data combined from both PH models and obtained with 4 transmit cycles. The correlation

coefficient in this case ranged from -0.71 to -0.79 (Table 3) and a statistically significant difference was seen between the subharmonic signal amplitudes obtained before and after inducing PH (Table 4). Finally, the relationship between absolute subharmonic signal amplitudes and portal vein pressures were used to track portal vein pressures in 2 other canines. The errors were lower when the SH_{All_Frames} were used as against the use of SH_{MIP} (0.2 to 1.9 mmHg vs. 1.8 to 6.9 mmHg) for 2 canines (Table 5); similar to the errors reported in a recent, cardiac SHAPE study conducted in canines (range: 0.2 to 2.5 mmHg; Dave et al. 2012a). Results from the cross-validation study indicate that the robustness of approximating the portal vein pressures using SHAPE (Table 6). The sensitivity, specificity and accuracy values for identifying clinically relevant PH (in canines) ranged from 67 to 85 % (Table 7). Thus, portal vein pressure monitoring using SHAPE appears to be feasible for testing clinical applications.

A major limitation of this study involves the use of fixed IAP levels for eliciting subharmonic emissions for SHAPE. This is reflected in the values presented in Table 7. For clinical applications, the optimization of IAP will be required on a case-by-case basis depending on body habitus, portal vein location and visualization, and other practical factors. Specifically, in a variable clinical population differences due to the attenuation, reverberation and aberration in the abdominal wall may make the promising results obtained in canines difficult to reproduce. However, these results do warrant a preliminary investigation in a clinical population to evaluate the usefulness of SHAPE in identifying PH. A real-time display of the subharmonic emissions as a function of IAP will allow the selection of optimum IAP levels (eliciting subharmonic emissions in the growth stage) for clinical SHAPE applications as well as future animal investigations. Also, discreet IAP levels were available on the ultrasound scanner. Thus, if the 'most-sensitive' IAP level for SHAPE falls between two consecutive discrete levels, then SHAPE's performance may not be optimum. Another practical problem before translating this technique into clinical applications arises from the fact that the subharmonic response depends on both the insonification IAP levels and ambient pressures. By displaying in real-time the subharmonic emissions as a function of IAP, the optimal IAP level can be identified, however, the associated subharmonic amplitude is still arbitrary due to variable attenuation and unknown ambient pressure. In other words, the same subharmonic amplitude measured in different subjects at an optimal IAP level (eliciting ambient pressure sensitive subharmonic emissions) could correspond to different ambient pressures. One approach to circumvent this problem may require obtaining the subharmonic gradient between the portal vein and the hepatic vein, which is analogous to the HVPG measurements used clinically (Eisenbrey et al. 2001b; 2011c). Further, the inability to operate in grayscale imaging mode during RF data acquisition may be addressed by the use of newly available dual and simultaneous B-mode and subharmonic imaging mode (Eisenbrey et al. 2011a, Dave et al 2012b). Another factor in this study was the mid-line abdominal incision created for accessing the main portal vein to obtain reference portal vein pressures; but absolute portal vein pressures cannot be obtained otherwise.

Sonazoid microbubbles have previously shown ambient pressure sensitivity of -6.58 mmHg/dB (Andersen and Jensen 2009) in simulation studies, -13.98 mmHg/dB (Halldorsdottir et al. 2011) in static tank experiments with single element transducers and -10.88 mmHg/dB (Dave et al. 2011) for *in vitro* flow phantom studies with commercially available ultrasound scanner. Note that the experimental sensitivity values are quite close to each other in the controlled *in vitro* setup, even though one of the studies used single element transducer while the other used a commercial scanner. Further, two separate *in vivo* studies conducted 7 years apart (to the best of our knowledge, the only two *in vivo* studies published on subharmonic aided pressure estimation to date) have reported the sensitivity values of about -4.44 mmHg/dB (Forsberg et al. 2005) with single element transducers and about -4.92

mmHg/dB (Dave et al. 2012a) with a commercial unit. In this study, that also used a commercially available ultrasound scanner and probe, the ultrasound scanning was performed after mid-line abdominal incision. This lack of attenuation may have contributed to the observed lower gradient in the range of -1.44 to -1.69 mmHg/dB than would be expected if scanning was performed through an intact abdomen. Interestingly studies with phospholipid-shell microbubbles engineered with optimized initial surface tension have reported a sensitivity of 2.12 mmHg/dB (Frinking et al. 2010). But such lab-engineered microbubbles may require further research and safety studies prior to clinical use.

An accurate theoretical explanation governing the decrease in subharmonic emissions from UCAs as a function of an increase in ambient pressures is currently lacking (Katiyar et al. 2011). However, empirical evidence (Shi et al. 1999) and other independent studies (Adam et al. 2005; Andersen and Jensen 2010) have reported the same effect. For the purpose of subharmonic imaging, it was shown that relatively low threshold values (0.02 - 0.15 MPa; ≤ levels corresponding to 10 % IAP level considered in this study) are required to elicit subharmonic emissions from microbubbles closest to their buckling state (Frinking et al. 2010). This buckling state is characterized by zero (minimal) initial surface tension and, thus, specific bubbles engineered with zero initial surface tension may be useful to extract this relationship for subharmonic imaging (Frinking et al. 2010). Alternately, a different approach was proposed in another study where low ambient pressure modulations in the microbubbles' vicinity may be established, that possibly drive the microbubbles to their buckling state by altering the surface tension values and consequently lead to emission of a relatively higher subharmonic signal at relatively lower IAP (Faez et al. 2011). These studies indicate that the subharmonic emissions may be tailored for subharmonic imaging, but *in vivo* applications were not implemented (Frinking et al. 2010; Faez et al. 2011). Besides, in the study presented here the subharmonic emissions at 10 % IAP were too low to be separated from the ambient noise level. Thus, the *in vivo* application of using even lower IAP values to elicit a stronger subharmonic signal *in vivo* remains technically challenging.

In two separate *in vitro* studies (Biagi et al. 2007, Frinking et al. 2010) using in-house manufactured microbubbles and also SonoVue (Bracco, Milan, Italy), it was shown that subharmonic emissions may be characterized by five stages, namely, occurrence, growth, stabilization, regrowth and saturation. Comparing the IAP levels considered in the current study with the levels used *in vitro* (Biagi et al. 2007, Frinking et al. 2010), it may be surmised that the subharmonic emissions in this study may correspond to the regrowth phase. However, major differences exist between these two referenced studies and the current study. The microbubbles used here were different (Sonazoid) and the current study was conducted *in vivo*, while the two other studies are based on behavior of the microbubbles *in vitro* where an idealized setup permits known peak negative acoustic pressures on the microbubbles and control over ambient pressures. *In vivo*, conditions depart markedly from this idealized *in vitro* setup; in this study only ambient noise was observed at IAP levels of 10 % (corresponding to the occurrence stage in Shi et al. 1999), whereas a reasonable subharmonic at IAP levels of 20 % and 40 % (corresponding to the growth stage in Shi et al. 1999). Also, explicit analysis with Sonazoid microbubbles (which were used in this study) *in vitro* using a test setup mentioned elsewhere (Halldorsdottir et al. 2011) revealed only the occurrence, growth and saturation phases as described previously (Shi et al. 1999). This may indicate that the 5 stages of subharmonic emissions may be a characteristic of the in-house manufactured microbubbles (as in Frinking et al. 2010), which were not accessible to us, or of SonoVue microbubbles which are different in composition with respect to Sonazoid microbubbles used in this study – also there have been no observations (to the best of our knowledge) reported on these 5 stages of subharmonic emissions from microbubbles *in vivo*, whereas implications of the 3 stages of subharmonic

emissions have been seen and utilized for ambient pressure estimation *in vivo* (Dave et al. 2011, 2012a).

For PH detection and monitoring, catheter based HVPG measurements are the gold standard. As this HVPG measurement technique is invasive, there are several other noninvasive techniques being developed either to estimate HVPG and detect PH and/or cirrhosis (the leading cause of PH in the Western world (Cokkinos and Dourakis 2009)). Techniques to measure liver tissue stiffness as a measure of cirrhosis (Vizzutti et al. 2007) and/or fibrosis or splenic stiffness (using MRI) as an indirect indicator of PH (Talwalkar et al. 2009) have been proposed. The liver stiffness measurements (LSMs) correlated weakly with HVPG (r^2 =.17) for patients with severe PH and are not obtainable for patients with ascites, nonalcoholic fatty liver disease and patients with high body-mass-index (BMI > 35) (Vizzutti et al. 2007), A recent study showed that the heart rate, cardiac index and baroreceptor sensitivity weakly correlated with HVPG measurements (r^2 ranging from 0.28 to 0.48); but the optimal cut-offs remain to be defined for predicting clinically significant PH (Rye et al. 2011). The use of ultrasound to assess several indirect measures predicting PH like portal vein diameter and flow, hepatic artery and vein flow, subjective evaluation of liver morphology, splenic size, portosystemic collateral and ascites has also been studied (Cokkinos and Dourakis 2009). Unfortunately portal vein diameter and flow patterns vary even in PH states, due to differential development of portosystemic shunts and collateral circulation in patients (Lafortune et al. 1984; Cokkinos and Dourakis 2009). Other studies have reported on the use Doppler ultrasound of the hepatic vein and some Doppler derived indices to monitor portal vein pressures indirectly but results have been mixed (Baik et al. 2006; Kim et al. 2007; Kim et al. 2011). The safety of a different approach combining endoscopy and portal vein pressure measurements was proved in a porcine model, however no simultaneous pressure measurements were obtained to validate this method (Giday et al. 2008).

Above all, the current standard of direct hepatic venous catheterization should be substituted by a noninvasive, accurate and reliable method to estimate HVPG or portal vein pressures (Thabut et al. 2011). Such a method would allow screening, diagnosis, monitoring and prognosis of chronic liver diseases or cirrhosis and would limit the number of endoscopies performed (especially for screening populations or patients without clinical signs of PH). Our work documents that the SHAPE technique may be used to track portal vein pressures and thus, may be useful as a screening tool for portal vein pressure monitoring. Recently, we have presented preliminary findings of a similar approach to identify PH in a clinical population and our results revealed a correlation of 0.81 between the HVPG and the subharmonic gradient, when based on data from 27 patients and, this correlation improved to 0.86 when the study included data from 37 patients (Eisenbrey et al. 2011b, 2011c). These preliminary results in a very limited patient population corroborate the findings of the results presented in the current manuscript. The complete results of the patient study will be published in the future.

CONCLUSION

The efficacy of SHAPE to determine portal vein pressures and monitor changes in portal vein pressures in the canine PH models considered here has been proven. For “optimum” insonification, the changes in subharmonic signal amplitude correlated with changes in portal vein pressures; correlation coefficient ranged from -0.82 to -0.94 and from -0.70 to -0.73 for PH models considered separately or together, respectively. The subharmonic signal amplitudes correlated with absolute portal vein pressures (r: -0.71 to -0.79). There was a statistically significant difference between subharmonic amplitudes before and after inducing PH ($p \leq 0.01$). Portal vein pressures estimated using SHAPE did not reveal

significant differences ($p>0.05$) with respect to the pressures obtained using the Millar pressure catheter. The efficacy of this approach under the variable conditions encountered in a real clinical setting will ultimately determine its usefulness. Nonetheless, based on the results presented in the controlled PH models considered here, SHAPE may in the future become a viable clinical tool for measuring portal vein pressures and monitoring treatment in symptomatic or critically ill cirrhotic patients, and for identifying nascent PH in asymptomatic patients.

Acknowledgments

This study was supported by National Institutes of Health grants R21 HL081892 and RC1 DK087365 (supporting JRE); and US Army Medical Research & Material Command grant W81XWH-08-1-0503 (supporting VGH). The authors acknowledge the support of GE Healthcare, Oslo, Norway for supplying Sonazoid.

References

Abraldes JG, Pasarin M, Garcia-Pagan JC. Animal models of portal hypertension. World J Gastroenterol. 2006; 12:6577–84. [PubMed: 17075968]

Adam D, Sapunar M, Burla E. On the relationship between encapsulated ultrasound contrast agent and pressure. Ultrasound Med Biol. 2005; 31:673–86. [PubMed: 15866417]

Andersen KS, Jensen JA. Ambient pressure sensitivity of microbubbles investigated through a parameter study. J Acoust Soc Am. 2009; 126:3350–8. [PubMed: 20000949]

Andersen KS, Jensen JA. Impact of acoustic pressure on ambient pressure estimation using ultrasound contrast agent. Ultrasonics. 2010; 50:294–9. [PubMed: 19822339]

Baik SK, Kim JW, Kim HS, Kwon SO, Kim YJ, Park JW, Kim SH, Chang SJ, Lee DK, Han KH, Um SH, Lee SS. Recent variceal bleeding: Doppler US hepatic vein waveform in assessment of severity of portal hypertension and vasoactive drug response. Radiology. 2006; 240:574–80. [PubMed: 16864678]

Biagi E, Breschi L, Vannacci E, Masotti L. Stable and transient subharmonic emissions from isolated contrast agent microbubbles. IEEE Trans Ultrason Ferroelectr Freq Control. 2007; 54:480–97. [PubMed: 17375818]

Bland JM, Altman DG. Multiple significance tests: the Bonferroni method. BMJ. 1995; 310:170. [PubMed: 7833759]

Bouakaz A, de Jong N. WFUMB Safety Symposium on Echo-Contrast Agents: nature and types of ultrasound contrast agents. Ultrasound Med Biol. 2007; 33:187–96. [PubMed: 17223253]

Bouakaz A, Frinking PJ, de Jong N, Bom N. Noninvasive measurement of the hydrostatic pressure in a fluid-filled cavity based on the disappearance time of micrometer-sized free gas bubbles. Ultrasound Med Biol. 1999; 25:1407–15. [PubMed: 10626628]

Buob S, Johnston AN, Webster CR. Portal hypertension: pathophysiology, diagnosis, and treatment. J Vet Intern Med. 2011; 25:169–86. [PubMed: 21382073]

Chen Y, Zhang Q, Liao Y, Guo F, Zhang Y, Zeng Q, Jin W, Shi H, Zhou M. A modified canine model of portal hypertension with hypersplenism. Scand J Gastroenterol. 2009; 44:478–85. [PubMed: 19096979]

Cokkinos DD, Dourakis SP. Ultrasonographic assessment of cirrhosis and portal hypertension. Current Medical Imaging Reviews. 2009; 5:62–70.

D'Amico G, Garcia-Tsao G, Pagliaro L. Natural history and prognostic indicators of survival in cirrhosis: a systematic review of 118 studies. J Hepatol. 2006; 44:217–31. [PubMed: 16298014]

Dave J, Halldorsdottir V, Eisenbrey J, Liu JB, McDonald M, Dickie K, Leung C, Forsberg F. Noninvasive estimation of dynamic pressures in vitro and in vivo using the subharmonic response from microbubbles. IEEE Trans Ultrason Ferroelectr Freq Control. 2011; 58:2056–66. [PubMed: 21989870]

Dave JK, Forsberg F, Fernandes S, Piccoli CW, Fox TB, Merton DA, Leodore LM, Hall AL. Static and dynamic cumulative maximum intensity display mode for subharmonic breast imaging: a

comparative study with mammographic and conventional ultrasound techniques. J Ultrasound Med. 2010; 29:1177–85. [PubMed: 20660451]

Dave JK, Halldorsdottir VG, Eisenbrey JR, Raichlen JS, Liu JB, McDonald ME, Dickie K, Wang S, Leung C, Forsberg F. Noninvasive LV Pressure Estimation Using Subharmonic Emissions From Microbubbles. JACC: Cardiovascular Imaging. 2012a; 5:87–92. [PubMed: 22239898]

Dave J, Halldorsdottir V, Eisenbrey J, Park S, Dianis S, Chalek C, Merton D, Liu J, Machado P, Thomenius K, Brown D, Forsberg F. Automated power optimization for subharmonic aided pressure estimation. J Ultrasound Med. 2012b; 31(suppl):S44.

Eisenbrey JR, Dave JK, Halldorsdottir VG, Merton DA, Machado P, Liu JB, Miller C, Gonzalez JM, Park S, Dianis S, Chalek CL, Thomenius KE, Brown DB, Navarro V, Forsberg F. Simultaneous grayscale and subharmonic ultrasound imaging on a modified commercial scanner. Ultrasonics. 2011a; 51:890–7. [PubMed: 21621239]

Eisenbrey, JR.; Gonzalez, JM.; Dave, JK.; Halldorsdottir, VG.; Merton, DA.; Machado, P.; Miller, C.; Park, S.; Dianis, S.; Chalek, CL.; Thomenius, KE.; Brown, DB.; Forsberg, F.; Navarro, V. Noninvasive subharmonic aided pressures estimation (SHAPE) of portal hypertension: Initial Clinical Results. Presented at The Liver Meeting; 2011b. (Abstract), 10 AM EST: (http://liverlearning.aasld.org/aasld/2011/thelivermeeting/13605/undefined)

Eisenbrey JR, Dave JK, Halldorsdottir VG, Merton DA, Machado P, Miller C, Gonzalez JM, Park S, Dianis S, Chalek CL, Thomenius KE, Brown DB, Navarro V, Forsberg F. Subharmonic aided pressure estimation in patients with suspected portal hypertension. Proc IEEE Ultrason Symp. 2011c:620–3. Abstract.

Faez T, Renaud G, Defontaine M, Calle S, de Jong N. Dynamic manipulation of the subharmonic scattering of phospholipid-coated microbubbles. Phys Med Biol. 2011; 56:6459–73. [PubMed: 21934190]

Fairbank WM Jr, Scully MO. A new noninvasive technique for cardiac pressure measurement: resonant scattering of ultrasound from bubbles. IEEE Trans Biomed Eng. 1977; 24:107–10. [PubMed: 892812]

Field, A. Discovering statistics using SPSS. 3. London: SAGE publications Ltd; 2009. Discovering statistics using SPSS; p. 822

Forsberg F, Liu JB, Shi WT, Furuse J, Shimizu M, Goldberg BB. In vivo pressure estimation using subharmonic contrast microbubble signals: proof of concept. IEEE Trans Ultrason Ferroelectr Freq Control. 2005; 52:581–3. [PubMed: 16060506]

Forsberg F, Piccoli CW, Merton DA, Palazzo JJ, Hall AL. Breast lesions: imaging with contrast-enhanced subharmonic US--initial experience. Radiology. 2007; 244:718–26. [PubMed: 17690324]

Frinking PJ, Brochot J, Arditi M. Subharmonic scattering of phospholipid-shell microbubbles at low acoustic pressure amplitudes. IEEE Trans Ultrason Ferroelectr Freq Control. 2010; 57:1762–71. [PubMed: 20704062]

Ganor Y, Adam D, Kimmel E. Time and pressure dependence of acoustic signals radiated from microbubbles. Ultrasound Med Biol. 2005; 31:1367–74. [PubMed: 16223640]

Giday SA, Clarke JO, Buscaglia JM, Shin EJ, Ko CW, Magno P, Kantsevoy SV. EUS-guided portal vein catheterization: a promising novel approach for portal angiography and portal vein pressure measurements. Gastrointest Endosc. 2008; 67:338–42. [PubMed: 18226699]

Goldberg B, Raichlen J, Forsberg F. Ultrasound Contrast Agents: Basic Principles and Clinical Applications. Martin Dunitz. 2001

Halldorsdottir VG, Dave JK, Leodore LM, Eisenbrey JR, Park S, Hall AL, Thomenius K, Forsberg F. Subharmonic contrast microbubble signals for noninvasive pressure estimation under static and dynamic flow conditions. Ultrason Imaging. 2011; 33:153–64. [PubMed: 21842580]

Halpern EJ. Noninvasive assessment of portal hypertension - can US aid in the prediction of portal pressure and monitoring of therapy? Radiology. 2006; 240:309–10. [PubMed: 16864661]

Hök B. A new approach to noninvasive manometry: interaction between ultrasound and bubbles. Med Biol Eng Comput. 1981; 19:35–9. [PubMed: 7278405]

Iezzi R, Basilico R, Giancristofaro D, Pascali D, Cotroneo AR, Storto ML. Contrast-enhanced ultrasound versus color duplex ultrasound imaging in the follow-up of patients after endovascular abdominal aortic aneurysm repair. J Vasc Surg. 2009; 49:552–60. [PubMed: 19135839]

Jenkins HP, Janda R. Studies on the use of gelatin sponge or foam as an hemostatic agent in experimental liver resections and injuries to large veins. Ann Surg. 1946; 124:952–61.

Jin W, Deng L, Zhang Q, Lin D, Zhu J, Chen Y, Chen B, Li J. A canine portal hypertension model induced by intra-portal administration of Sephadex microsphere. J Gastroenterol Hepatol. 2010; 25:778–85. [PubMed: 20492334]

Katiyar A, Sarkar K, Forsberg F. Modeling subharmonic response from contrast microbubbles as a function of ambient static pressure. J Acoust Soc Am. 2011; 129:2325–35. [PubMed: 21476688]

Kim MY, Baik SK, Park DH, Lim DW, Kim JW, Kim HS, Kwon SO, Kim YJ, Chang SJ, Lee SS. Damping index of Doppler hepatic vein waveform to assess the severity of portal hypertension and response to propranolol in liver cirrhosis: a prospective nonrandomized study. Liver Int. 2007; 27:1103–10. [PubMed: 17845539]

Kim SY, Jeong WK, Kim Y, Heo JN, Kim MY, Kim TY, Sohn JH. Changing waveform during respiration on hepatic vein Doppler sonography of severe portal hypertension: comparison with the damping index. J Ultrasound Med. 2011; 30:455–62. [PubMed: 21460144]

Lafortune M, Marleau D, Breton G, Viallet A, Lavoie P, Huet PM. Portal venous system measurements in portal hypertension. Radiology. 1984; 151:27–30. [PubMed: 6701328]

Landmark KE, Johansen PW, Johnson JA, Johansen B, Uran S, Skotland T. Pharmacokinetics of perfluorobutane following intravenous bolus injection and continuous infusion of sonazoid in healthy volunteers and in patients with reduced pulmonary diffusing capacity. Ultrasound Med Biol. 2008; 34:494–501. [PubMed: 18096304]

Lebrec D, Sogni P, Vilgrain V. Evaluation of patients with portal hypertension. Baillieres Clin Gastroenterol. 1997; 11:221–41. [PubMed: 9395745]

Mac DS, Matthews WH. Fibrin foam and gelfoam in experimental kidney wounds. J Urol. 1947; 57:802–11. [PubMed: 20295849]

Miwa, H. Pressure measuring system with ultrasonic wave. U S Patent. 4,483,345. 1984.

Moan AS. The evaluation of liver dysfunction: when to suspect portal hypertension. JAAPA. 2009; 22:38–42. [PubMed: 19452820]

Navarro, VJ.; Rossi, S.; Herrine, SK. Pharmacology and Therapeutics: Principles to Practice. Saunders- Elsevier; 2008. Hepatic Cirrhosis; p. 505-26.

Palmaz JC, Garcia F, Sibbitt RR, Tio FO, Kopp DT, Schwesinger W, Lancaster JL, Chang P. Expandable intrahepatic portacaval shunt stents in dogs with chronic portal hypertension. Am J Roentgenol. 1986; 147:1251–4. [PubMed: 3490761]

Rye, K.; Mortimore, G.; Austin, A.; Freeman, J. Non-invasive assessment and prediction of clinically significant portal hypertension. Gut; Presented at the British Society of Gastroenterology Annual General Meeting; 2011. p. A245-6.abstract

Sanyal AJ, Bosch J, Blei A, Arroyo V. Portal hypertension and its complications. Gastroenterology. 2008; 134:1715–28. [PubMed: 18471549]

Seitchik MW, Poll M, Rosenthal W, Baronofsky ID. Studies in the hemodynamics following supradiaphragmatic constriction of the inferior vena cava. Ann Surg. 1961; 153:71–80. [PubMed: 13749816]

Shankar PM, Chapelon JY, Newhouse VL. Fluid pressure measurement using bubbles insonified by two frequencies. Ultrasonics. 1986; 24:333–6.

Shi WT, Forsberg F, Raichlen J, Needleman L, Goldberg G. Pressure dependence of subharmonic signals from contrast microbubbles. Ultrasound Med Biol. 1999; 25:275–83. [PubMed: 10320317]

Shi WT, Hoff L, Forsberg F. Subharmonic performance of contrast microbubbles: an experimental and numerical investigation. Proc of IEEE Ultrasonics Symposium. 2002; 2:1957–60.

Sontum PC. Physicochemical characteristics of Sonazoid, a new contrast agent for ultrasound imaging. Ultrasound Med Biol. 2008; 34:824–33. [PubMed: 18255220]

Sugita S, Ohnishi K, Saito M, Okuda K. Splanchnic hemodynamics in portal hypertensive dogs with portal fibrosis. Am J Physiol Gastrointest Liver Physiol. 1987; 252:G748–54.

Talwalkar JA, Yin M, Venkatesh S, Rossman PJ, Grimm RC, Manduca A, Romano A, Kamath PS, Ehman RL. Feasibility of in vivo MR elastographic splenic stiffness measurements in the assessment of portal hypertension. Am J Roentgenol. 2009; 193:122–7. [PubMed: 19542403]

Thabut D, Moreau R, Lebrec D. Noninvasive assessment of portal hypertension in patients with cirrhosis. Hepatology. 2011; 53:683–94. [PubMed: 21274889]

Vizzutti F, Arena U, Romanelli RG, Rega L, Foschi M, Colagrande S, Petrarca A, Moscarella S, Belli G, Zignego AL, Marra F, Laffi G, Pinzani M. Liver stiffness measurement predicts severe portal hypertension in patients with HCV-related cirrhosis. Hepatology. 2007; 45:1290–7. [PubMed: 17464971]

von Herbay A, Westendorff J, Gregor M. Contrast-enhanced ultrasound with SonoVue: differentiation between benign and malignant focal liver lesions in 317 patients. J Clin Ultrasound. 2010; 38:1–9. [PubMed: 19790253]

Yamana H, Yatsuka K, Kakegawa T. Experimental production of portal hypertension in dogs by a whole liver compression. Gastroenterol Jpn. 1983; 18:119–27. [PubMed: 6852438]

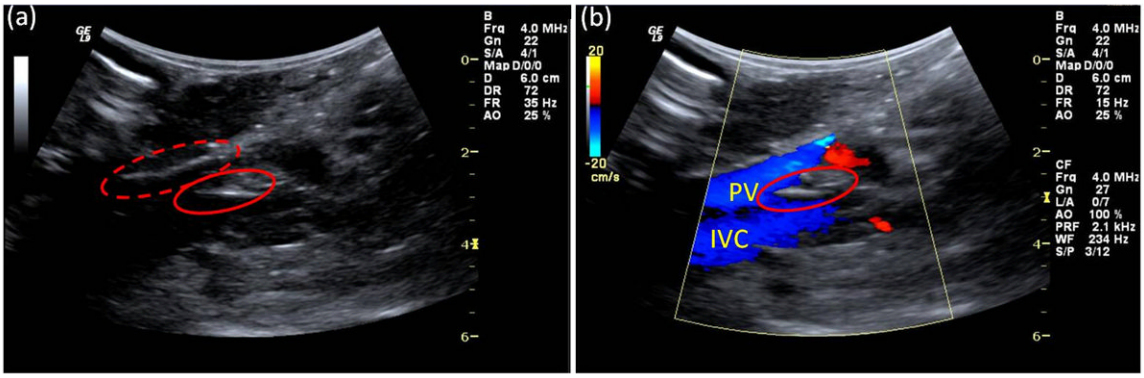

Fig. 1.

Grayscale B-mode and color Doppler images acquired during data acquisition. (a) The locations of the surgical inlet (red-dotted ring) and the pressure catheter (red ring) are indicated. (b) Color Doppler image verifying the presence of pressure catheter (red ring) in the portal vein (PV); inferior vena cava (IVC) is shown as well.

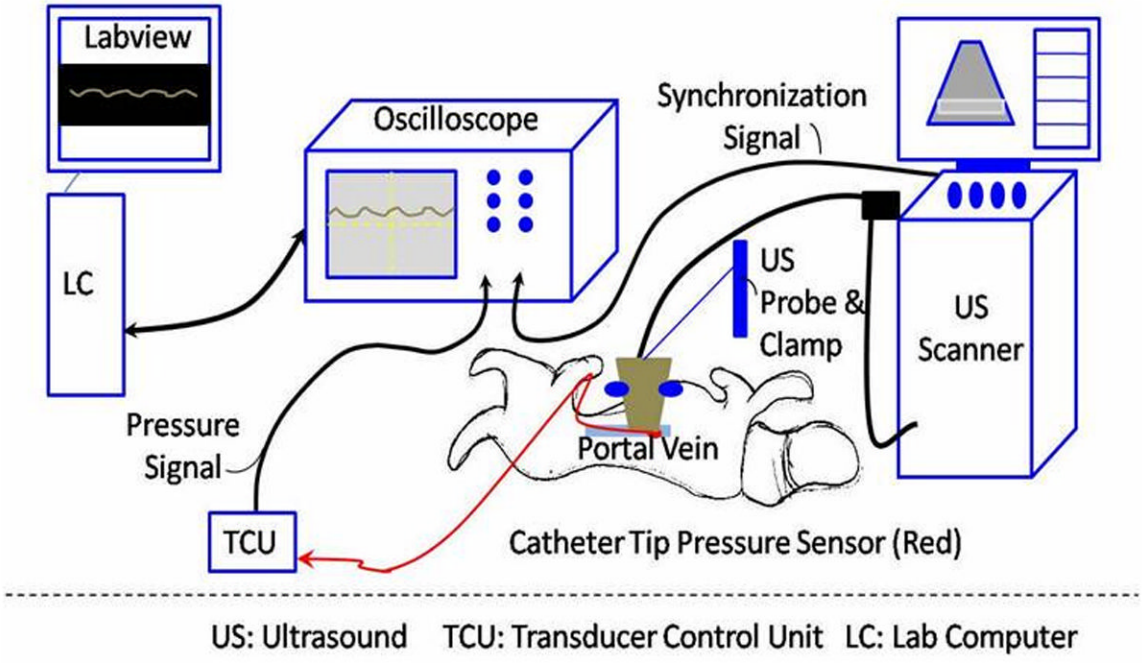

Fig. 2.
Schematic representing experimental setup.

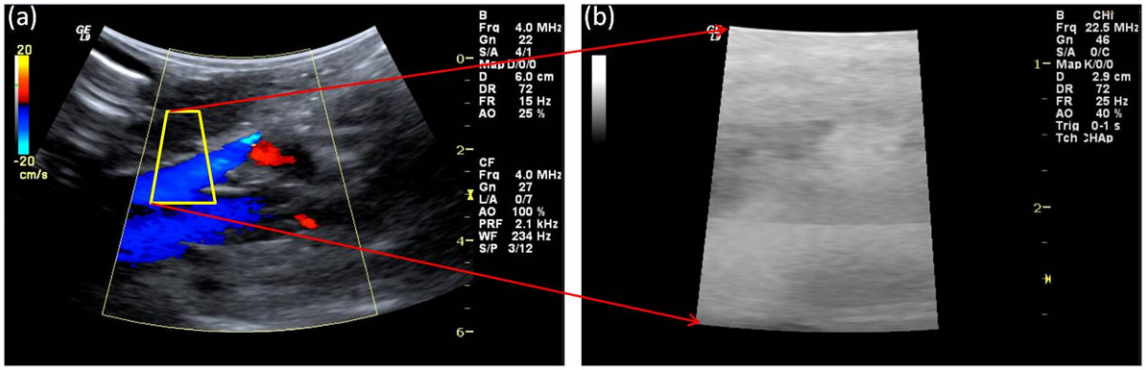

Fig. 3.

Data acquisition process. (a) Standard imaging mode where the ROI (region of interest with portal vein) is selected (yellow outline). (b) RF data acquisition mode.

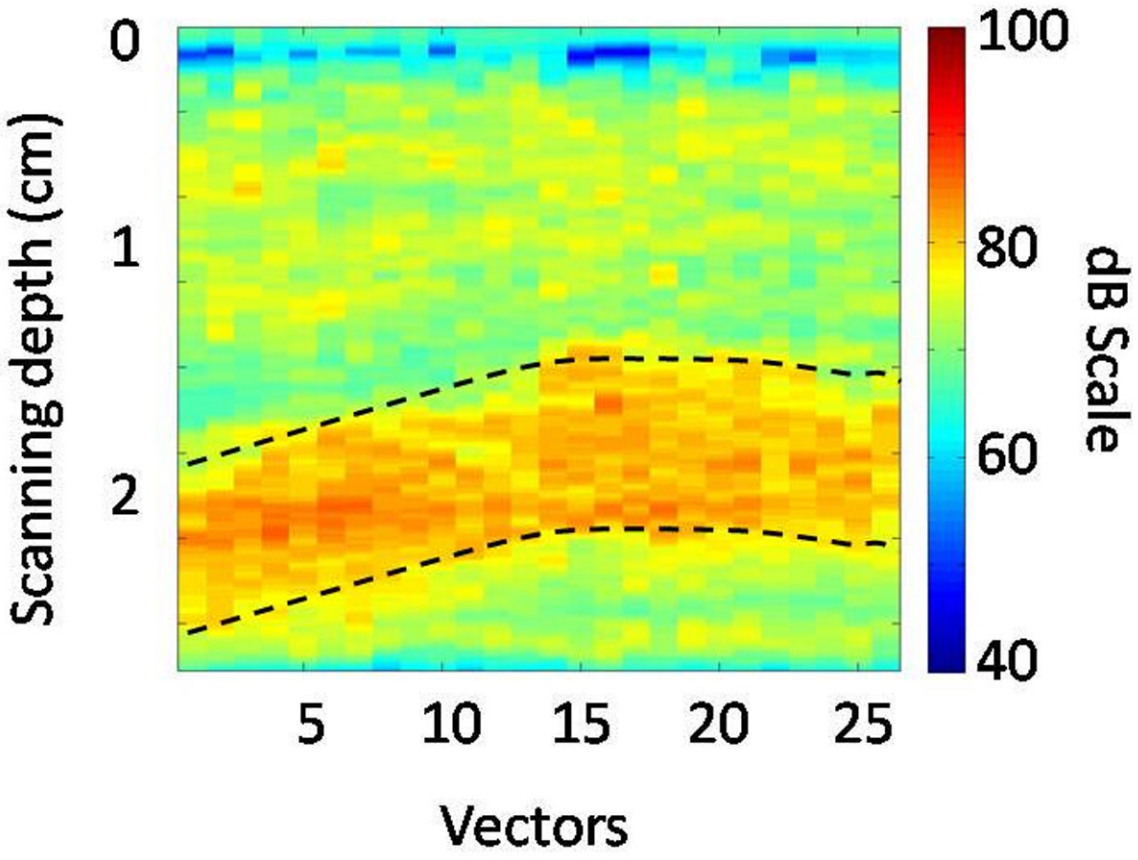

Fig. 4.

Maximum intensity projection (MIP) subharmonic image obtained from a canine. Note that the abscissa represents the width or the lateral span of the ROI shown in Fig. 3b. The dotted lines delineate the portal vein.

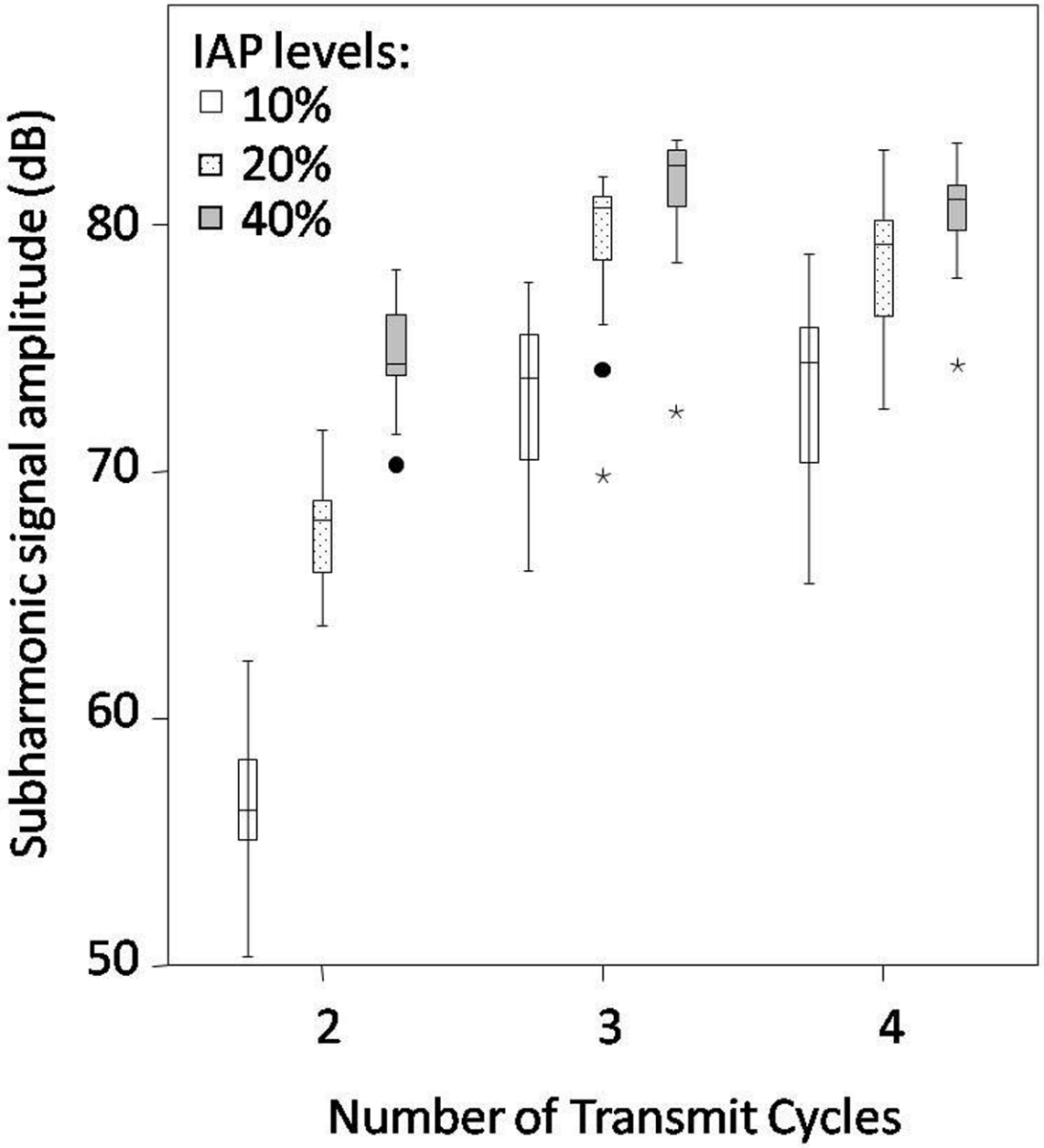

Fig. 5.

Boxplot of the subharmonic signal amplitudes obtained at 10 %, 20 % and 40 % incident acoustic power (IAP) levels with 2, 3 and 4 transmit cycles. Minor and major outliers are indicated with circles and asterisks, respectively. Note, that the subharmonic signal amplitudes obtained with 10 % IAP and with 2 cycles are relatively low as compared to the amplitudes obtained with 20 % and 40 % IAP, for 3 and 4 transmit cycles.

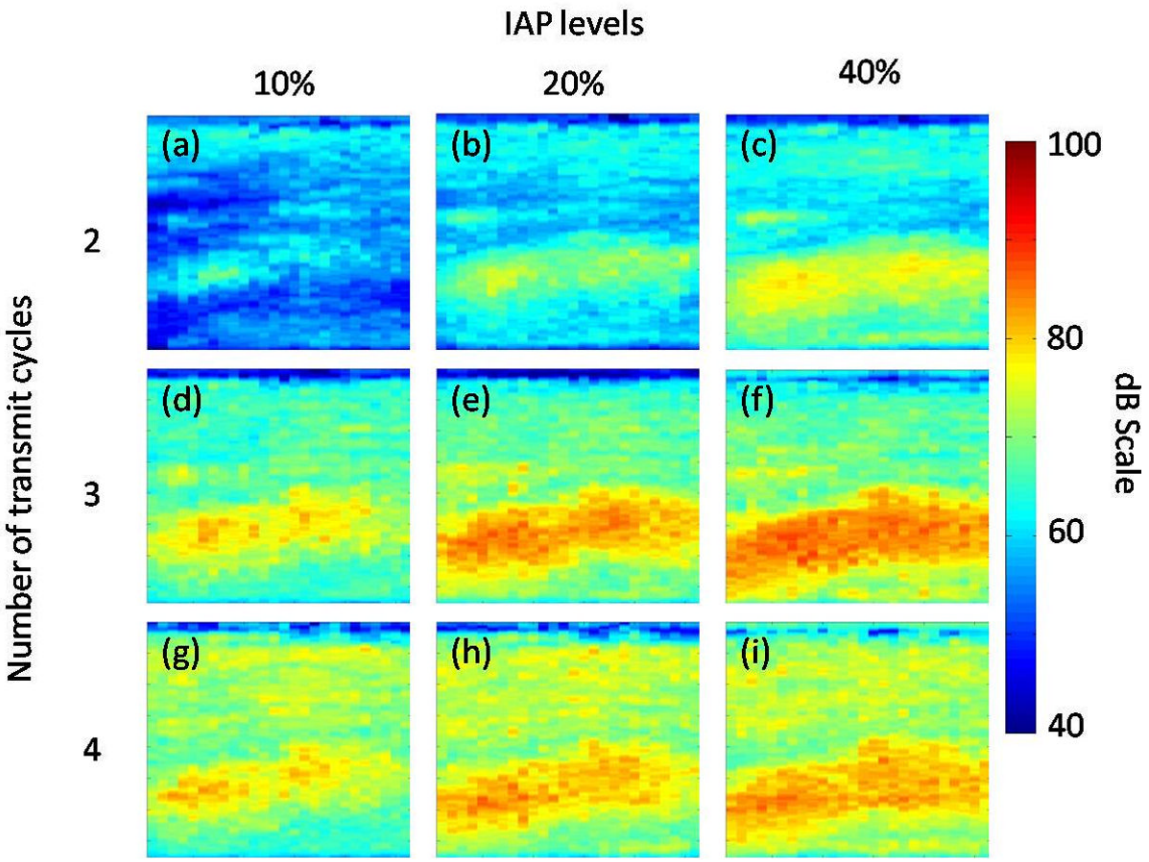

Fig. 6.

Maximum intensity projection (MIP) subharmonic images of the data obtained from ROI at 10 % (a, d, g), 20 %, (b, e, h) and 40 % (c, f, i) incident acoustic power (IAP) with 2 (a-c), 3 (d-f), and 4 (g-i) transmit cycles. Note, that subharmonic signal amplitude increases with an increase in IAP levels; but is relatively low for 2 transmit cycles.

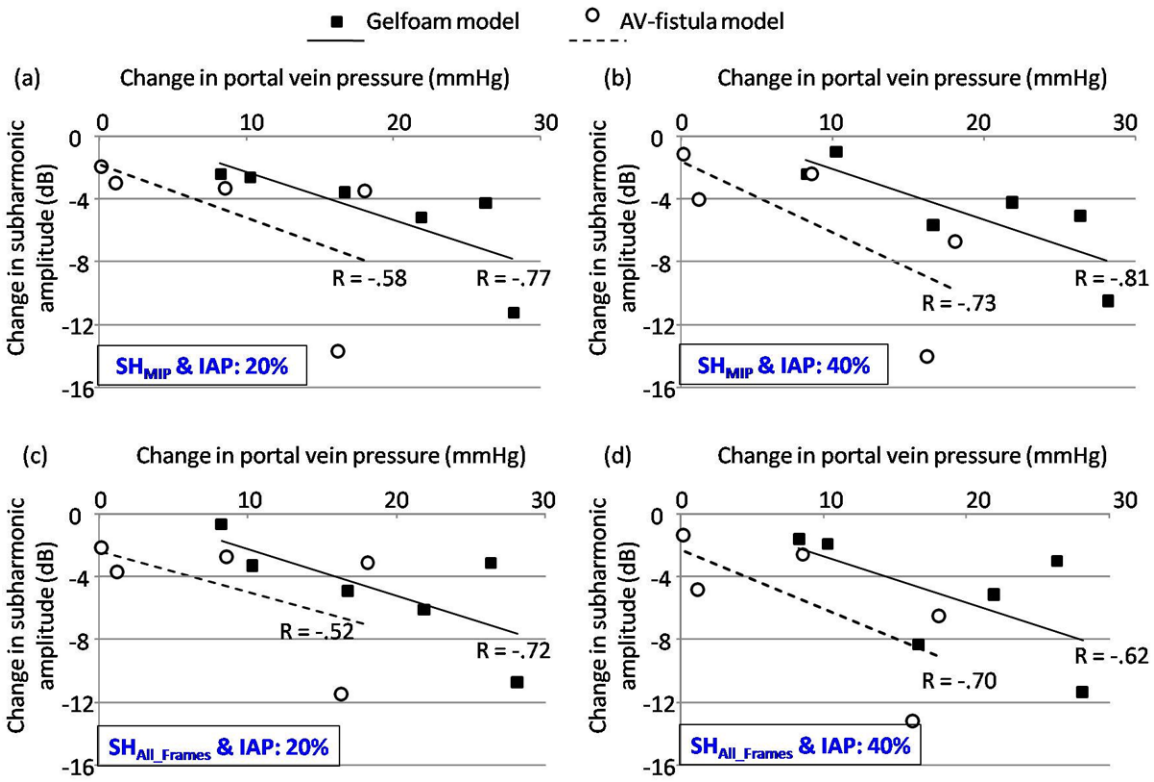

Fig 7.

Mean changes in the portal vein pressures are plotted with mean changes in subharmonic signal amplitudes acquired with 3 transmit cycles along with the best-fit line and the correlation coefficient is indicated for both the Gelfoam and AV-fistula portal hypertension models. (a) and (c) represent data acquired at 20 % incident acoustic power (IAP) levels for subharmonic signal analyzed from the MIP image (SH_{MIP}) and as the mean value from all the frames (SH_{All_Frames}), respectively. (b) and (d) represent the corresponding data acquired at 40 % IAP.

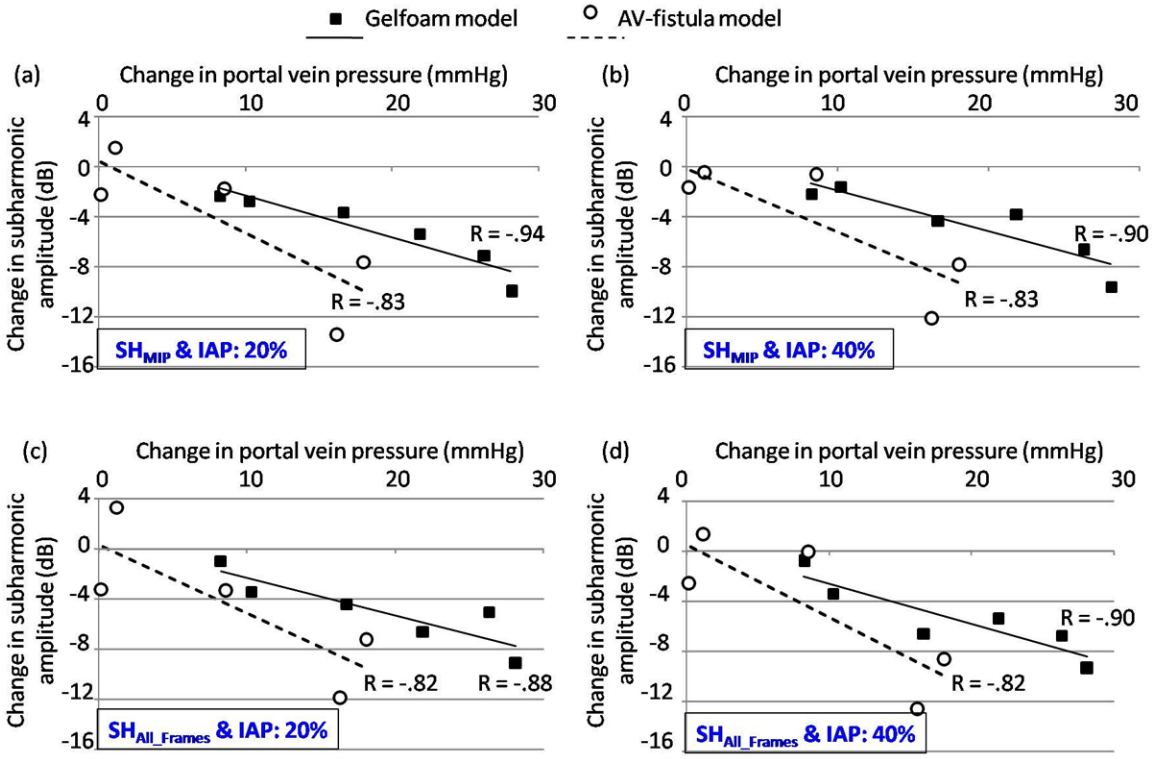

Fig 8.

Mean changes in the portal vein pressures are plotted with mean changes in subharmonic signal amplitudes acquired with 4 transmit cycles along with the best-fit line and the correlation coefficient is indicated for both the Gelfoam and AV-fistula portal hypertension models. (a) and (c) represent data acquired at 20 % incident acoustic power (IAP) for subharmonic signal analyzed from the MIP image (SH_{MIP}) and as the mean value from all the frames (SH_{All_Frames}), respectively. (b) and (d) represent the corresponding data acquired at 40 % IAP.

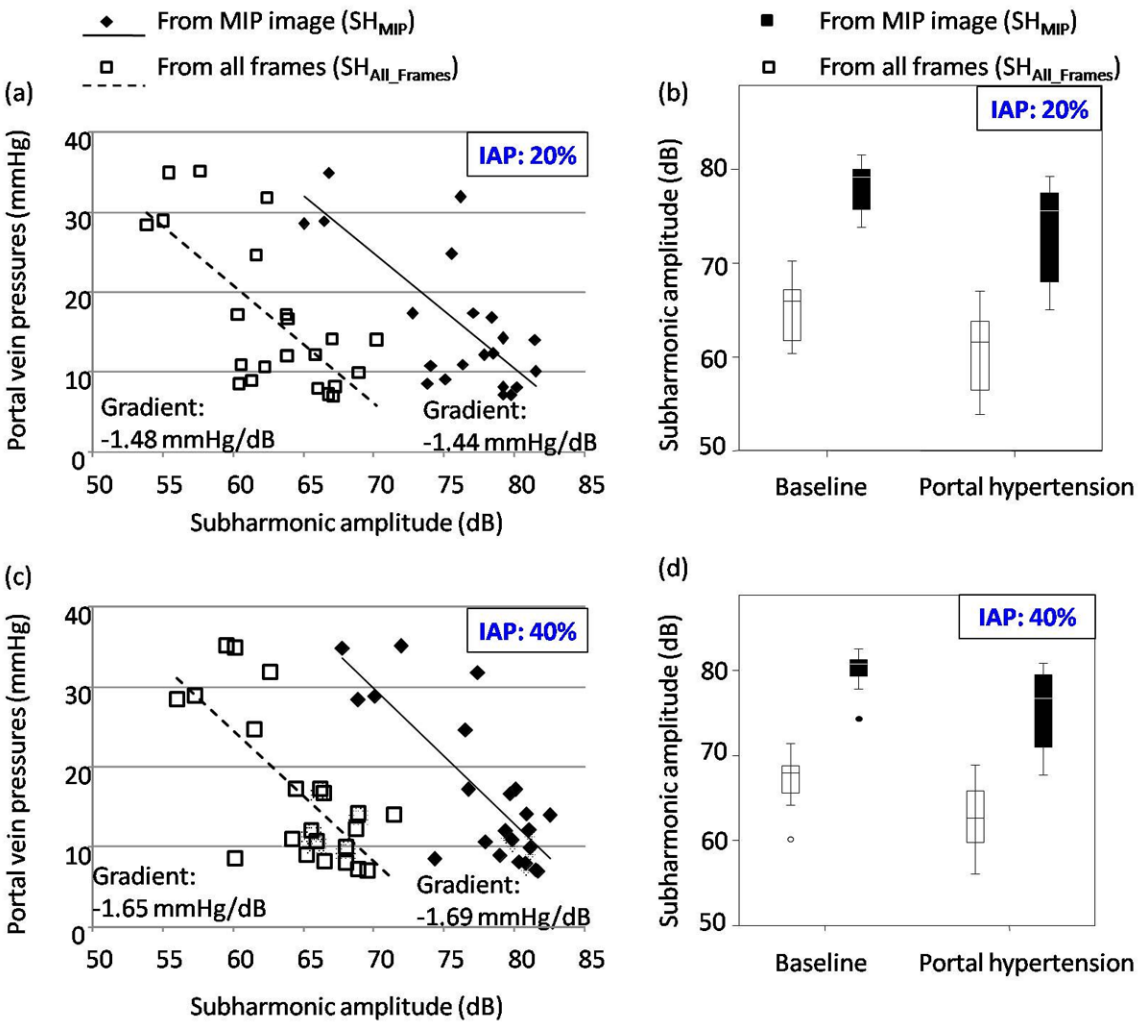

Fig 9.

Absolute portal vein pressures are plotted with absolute subharmonic signal amplitudes acquired with 4 transmit cycles (note, these are mean values obtained from each canine). (a-b) and (c-d) represent data acquired at 20 % and 40 % incident acoustic powers (IAPs), respectively. The subharmonic amplitudes obtained from the maximum intensity projection images (SH_{MIP}) and from the mean signal combined from all the frames (SH_{All_Frames}) are shown separately in each panel. The best-fit line along with its gradient is indicated in (a) and (c). Boxplots in (b) and (d) indicate the interquartile range (vertical span of the box), the median value (horizontal line within the box), the range (whiskers) and minor outliers (circles) for the subharmonic signal amplitudes. Note that the SH_{All_Frames} is relatively less than the SH_{MIP} (as expected).

Table 1

Portal vein pressures (mean pressures indicated with standard deviation).

	Minimum Pressure (mmHg)	Mean Pressure (mmHg)	Maximum Pressure (mmHg)
Baseline conditions (13 canines)*	5.6	9.4 ± 2.1	16.0
Gelfoam induced PH (6 canines)†	9.3	26.9 ± 8.3	36.7
AV-fistula induced PH (5 canines)†	8.8	19.1 ± 6.5	28.1

*Note that from 14 canines, for one canine technical difficulty associated with the pressure catheter impeded data acquisition; thus baseline data have been reported for 13 canines

†Single canine did not respond to treatment in each case resulting in data acquisition post portal hypertension (PH) from 6 canines in the Gelfoam group and 5 canines in the AV-fistula group

Table 2

Pearson's correlation coefficient (r) between the change in subharmonic signal and change in portal vein pressures when data from the Gelfoam and AV-fistula models were combined (n = 11)

Transmit Cycles	Incident Acoustic Power (%)	Subharmonic amplitudes from MIP image (SH_{MIP})		Subharmonic amplitudes from mean signal of all frames (SH_{All_Frames})	
		r	*p*-value	r	*p*-value
3	20	-0.53	0.094	-0.54	0.090
3	40	-0.56	0.071	-0.52	0.103
4	20	-0.72	0.013	-0.70	0.017
4	40	-0.70	0.016	-0.73	0.011

Table 3

Pearson's correlation coefficient (r) between absolute subharmonic signal amplitudes and absolute portal vein pressures when data from the Gelfoam and AV-fistula models were combined for 4 transmit cycles (n = 22)

Incident Acoustic Power (%)	Subharmonic amplitudes from MIP image (SH_{MIP})		Subharmonic amplitudes from mean signal of all frames (SH_{All_Frames})	
	r	***p*-value**	**r**	***p*-value**
20	-0.74	< 0.001	-0.71	< 0.001
40	-0.79	< 0.001	-0.73	< 0.001

Table 4

Paired t-test results when comparing subharmonic signal amplitudes obtained at baseline and portal hypertension conditions, with 4 transmit cycles (n = 11)

Incident Acoustic Power (%)	Subharmonic amplitudes from MIP image (SH_{MIP})			Subharmonic amplitudes from mean signal of all frames (SH_{All_Frames})		
	Mean Difference (dB)	95 % Confidence Interval of Difference (dB)	*p*-value	Mean Difference (dB)	95 % Confidence Interval of Difference (dB)	*p*-value
20	5.0	2.1-7.8	0.003	4.7	2.0-7.4	0.003
40	4.6	2.0-7.2	0.003	4.4	1.3-7.4	0.01

Ultrasound Med Biol. Author manuscript; available in PMC 2013 October 01.

Table 5

Predicting portal vein pressures and comparing with true pressures (true pressures were obtained with the Millar catheter)

Incident Acoustic Power (%)	From MIP image (SH_{MIP})			From mean signal of all frames (SH_{All_Frames})		
	Subharmonic amplitude (dB)	Calculated Pressure (mmHg)	True Pressure (mmHg)	Subharmonic signal (dB)	Calculated Pressure (mmHg)	True Pressure (mmHg)
Canine 1: Baseline						
20	80.2	10.1	8.0	68.5	8.2	8.0
40	81.8	9.8	8.0	69.8	8.5	8.0
Canine 2: Baseline						
20	85.4	2.6	7.8	67.5	9.7	7.8
40	87.0	0.9	7.8	69.5	9.0	7.8

Table 6

Comparing errors between true pressures obtained with Millar catheter and the pressures obtained with SHAPE data using cross-validation approach

Incident Acoustic Power (%)	Using data from MIP image (SH_{MIP}) SHAPE vs. catheter pressures			Using data from from mean signal of all frames (SH_{All_Frames}) SHAPE vs. catheter pressures		
	Mean Difference (mmHg)	95 % Confidence Interval of Difference (mmHg)	*p*-value	Mean Difference (mmHg)	95 % Confidence Interval of Difference (mmHg)	*p*-value
a) For all data						
20	-0.03	-3.0 to 3.0	0.982	-0.15	-3.4 to 3.1	0.924
40	0.08	-2.7 to 2.9	0.951	-0.09	-3.3 to 3.1	0.952
b) For baseline data only (before PH)						
20	3.47	-0.1 to 7.0	0.053	3.50	-0.9 to 7.9	0.110
40	3.23	-0.3 to 6.8	0.070	3.64	-0.9 to 8.2	0.103
c) For PH data only						
20	-3.5	-8.0 to 0.9	0.109	-3.8	-8.0 to 0.4	0.072
40	-3.1	-7.0 to 0.9	0.113	-3.8	-7.9 to 0.2	0.062

Table 7

Sensitivity, specificity and accuracy for detecting moderate through severe PH with a cut-off threshold for portal vein pressures of 16 mmHg (13 instances with portal vein pressures below 16 mmHg and 9 instances with portal vein pressures above 16 mmHg)

Incident Acoustic Power (%)	With SHAPE using SH_{MIP}			With SHAPE using SH_{All_Frames}		
	Sensitivity (%)	Specificity (%)	*Accuracy* (%)	Sensitivity (%)	Specificity (%)	*Accuracy* (%)
20	67	69	68	78	69	73
40	78	85	82	78	77	77